

# Metronomic scheduling of a cyclic hexapeptide Ra-VII for anti-angiogenesis, tumor vessel maturation and anti-tumor activity

Takayuki Koizumi,<sup>1,2</sup> Mayumi Abe,<sup>1,5</sup> Tohru Yamakuni,<sup>2</sup> Yasushi Ohizumi,<sup>2</sup> Yukio Hitotsuyanagi,<sup>3</sup> Koichi Takeya<sup>3</sup> and Yasufumi Sato<sup>1,4</sup>

<sup>1</sup>Department of Vascular Biology, Institute of Development, Aging, and Cancer, Tohoku University, 4-1 Seiryomachi, Aoba-ku, Sendai 980-8575; <sup>2</sup>Department of Pharmaceutical Molecular Biology, Graduate School of Pharmaceutical Science, Tohoku University, Aoba, Aramaki, Aoba-ku, Sendai 980-8578; and <sup>3</sup>School of Pharmacy, Tokyo University of Pharmacy and Life Science, 1432-1 Horinouchi, Hachioji, Tokyo 192-0392, Japan

(Received February 10, 2006/Revised March 22, 2006/Accepted March 26, 2006/Online publication May 9, 2006)

**RA-VII, a cyclic hexapeptide isolated from *Rubiae radix*, binds to actin, causing a conformational change in the actin molecule and inducing G<sub>2</sub> arrest by inhibiting cytokinesis. Here we examined the effect of RA-VII, its water-soluble derivative, and related RA-III and RA-V on endothelial cells. Among the four compounds tested, RA-VII most potently inhibited angiogenesis-related properties of endothelial cells (i.e. migration and proliferation) *in vitro*. We confirmed the anti-angiogenic activity of RA-VII *in vivo* by using a mouse corneal model. We then applied RA-VII for the treatment of tumors in mice. Daily intraperitoneal injection of RA-VII (1.5 or 3 mg/kg/day) exhibited no toxic effect on the animals, but significantly and dose dependently inhibited the growth of Lewis lung carcinoma cells previously inoculated into the mice. Interestingly, although two doses of RA-VII decreased the tumor vascular area to a similar extent, a higher dose of RA-VII led to tumor vessel maturation together with a significant increase in tumor cell apoptosis. Also, RA-VII showed a cytotoxic effect on Lewis lung carcinoma cells. These results indicate that metronomic scheduling of RA-VII is efficient for cancer treatment. A careful dose setting of RA-VII is crucial to obtain therapeutic superiority, possibly through tumor vessel maturation and a better distribution of the compound in the tumor tissue. (*Cancer Sci* 2006; 97: 665–674)**

Angiogenesis is the phenomenon by which blood vessels are newly formed from pre-existing vessels. Angiogenesis normally includes six sequential steps: detachment of mural pericytes for vascular destabilization, extracellular matrix degradation by endothelial proteases, migration of endothelial cells (EC), proliferation of EC, tube formation by EC, and reattachment of pericytes for vascular stabilization or maturation.<sup>(1)</sup> Angiogenesis is a physiological process observed during embryonic development, in the female reproductive system and in wound healing, but it also occurs under pathological conditions including cancer.<sup>(2)</sup> Vessels formed in cancer are immature and leaky because reattachment of pericytes is insufficient.<sup>(3)</sup>

The rationale to block angiogenesis as a treatment strategy for cancer was proposed more than 30 years ago.<sup>(4)</sup> The recent development of bevacizumab, a humanized antibody specific for vascular endothelial growth factor (VEGF), has

provided a major advance in the clinical field of anti-angiogenic therapy.<sup>(5)</sup> It is the first anti-angiogenic drug to be approved for the treatment of human cancer; however, there is still a limitation in its use. It has been shown to prolong survival only when given in combination with chemotherapy.<sup>(5)</sup> Thus, a number of other approaches are currently under development.<sup>(6)</sup>

The actin cytoskeleton system is involved in cell adhesion,<sup>(7)</sup> cell migration<sup>(8)</sup> and cell division.<sup>(9)</sup> It is well known that actin serves as the major component of stress fibers, which are formed during cell adhesion and cell migration.<sup>(7,8)</sup> In terms of cell division, actin filaments become concentrated in a contractile ring at the end of S phase. In the subsequent G<sub>2</sub> phase, this contractile ring constricts the cell at its mid region, forming an intracellular bridge between the two soon-to-be daughter cells and finally separates these cells.<sup>(9)</sup> The migration and proliferation are requisite properties of EC for angiogenesis.<sup>(1)</sup> Thus, actin can be a target for the regulation of angiogenesis. Indeed, we previously reported that actin-targeting goniodomin A, an antifungal polyether macrolide, exhibited anti-angiogenic activity.<sup>(10)</sup>

RA-VII is a cyclic hexapeptide isolated from *Rubiae radix*.<sup>(11)</sup> We recently showed it to bind to actin, causing a conformational change in the actin molecule and inducing G<sub>2</sub> arrest by inhibiting cytokinesis in cancer cells.<sup>(12)</sup> In the present study, we examined whether RA-VII would have anti-angiogenic activity and, if so, whether or not it would be effective for cancer treatment.

## Materials and Methods

### Materials

Materials and their sources were as follows: Dulbecco's modified Eagle's medium (DMEM), from Nissui Pharmaceutical Co. (Tokyo, Japan); basic fibroblast growth factor (bFGF), from Becton Dickinson Labware (Bedford, MA, USA); VEGF<sub>165</sub>, from Sigma (St Louis, MO, USA); penicillin/streptomycin,

<sup>4</sup>To whom correspondence should be addressed.  
E-mail: y-sato@idac.tohoku.ac.jp

<sup>5</sup>Present address: Department of Nanomedicine, Tokyo Medical and Dental University Graduate School, 1-5-45 Yushima, Bunkyo-ku, Tokyo 113-8519, Japan.

from Dainippon Pharmaceutical Co. (Osaka, Japan); fetal bovine serum (FBS), from JRH Biosciences (Lenexa, KS, USA); Tetra Color ONE, from Seikagaku (Tokyo, Japan); Type I-A collagen, from Nitta Gelatin (Osaka, Japan); rhodamine-conjugated phalloidin and 4',6-diamidino-2-phenylindole dihydrochloride (DAPI), from Molecular Probes (Eugene, OR, USA); rat antimouse CD31 monoclonal antibody, from Research Diagnostics (Flanders, NJ, USA); proteinase K and Non-Specific Staining Blocking Reagent, from Dako Cytomation (Glostrup, Denmark); goat antirat IgG conjugated to biotin, from Vector Laboratories (Burlingame, CA, USA); goat antimouse IgG conjugated to fluorescein-isothiocyanate (FITC), from Chemicon (Temecula, CA, USA); TdT, from Invitrogen (Carlsbad, CA, USA); and fluorescein-12-dUTP, from Roche Diagnostics (Penzberg, Germany). RA-VII, its water-soluble derivative, and RA-III and RA-V were described previously.<sup>(11,12)</sup> The chemical structures of these compounds are shown in Fig. 1. All other reagents used were from Sigma or Wako (Osaka, Japan).

#### Preparation of cyclic hexapeptides for use in experiments

For *in vitro* studies, RA-VII, RA-III and RA-V were dissolved in dimethylsulfoxide, and the water-soluble derivative of RA-VII was dissolved in distilled water, to yield 10 mM stock solutions, which were aliquoted and stored at  $-20^{\circ}\text{C}$ . For experiments the aliquots were additionally diluted

in working medium at the concentrations indicated in the figure legends. For *in vivo* studies, RA-VII was prepared in gum arabic in phosphate-buffered saline (PBS; 0.5%) and administered at the doses indicated in the figure legends.

#### Cell culture

Bovine aortic endothelial cells (BAEC) and Lewis lung carcinoma (LLC) cells were cultured in DMEM supplemented with 10% FBS, 100  $\mu\text{g}/\text{mL}$  penicillin, 100  $\mu\text{g}/\text{mL}$  streptomycin and 4 mM L-glutamine (10% FBS-DMEM). Human umbilical vein endothelial cells (HUVEC) were cultured on type-I collagen-coated dishes (IWAKI, Tokyo, Japan) in endothelial basal medium (EBM) containing endothelial cell growth supplements and 10% FBS.

#### Proliferation

Aliquots of BAEC ( $1 \times 10^4$ ) or HUVEC ( $1 \times 10^4$ ) were plated in a 96-well plate and cultured in 10% FBS-DMEM for 24 h. In the case of BAEC, the medium was changed to 0.1% bovine serum albumin (BSA) in DMEM (BSA-DMEM) with or without 1 nM bFGF and the desired concentrations of RA-VII, RA-III, RA-V or water-soluble derivative. In the case of HUVEC, the medium was changed to 1% FBS in DMEM with or without 1 nM VEGF and the desired concentrations of RA-VII, RA-III, RA-V or water-soluble derivative. After a 72 h incubation, the cells were incubated with Tetra Color ONE for 4 h. Absorbance was then read at 450 nm.

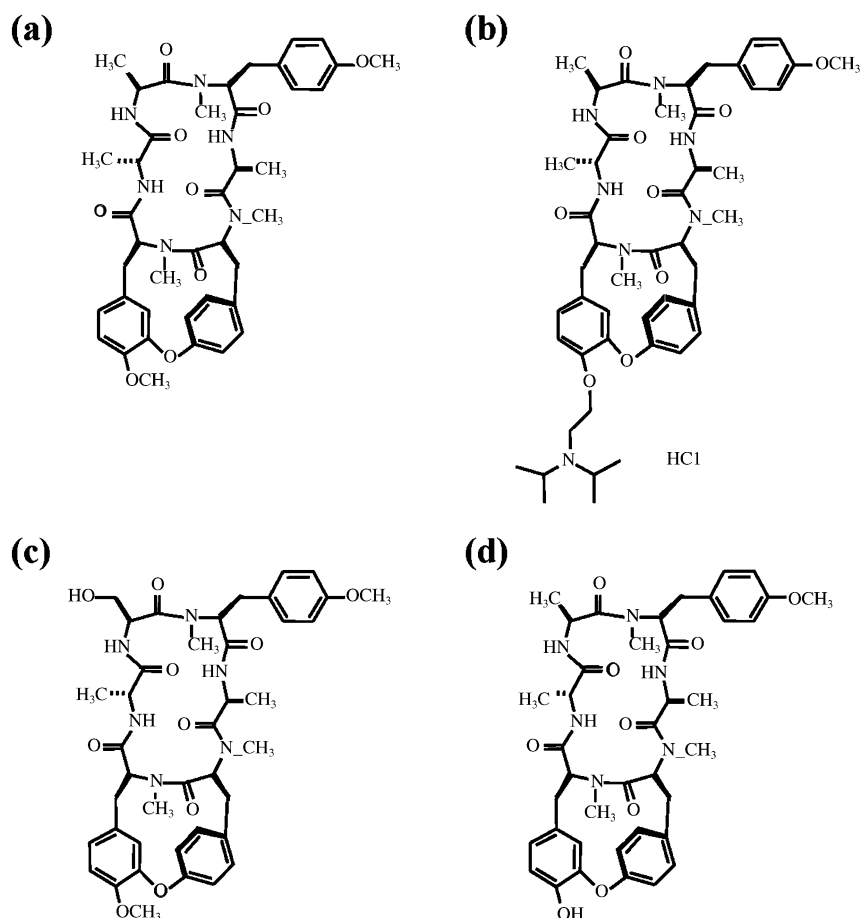


**Fig. 1.** Chemical structures of (a) RA-VII, (b) its water-soluble derivative and related (c) RA-III and (d) RA-V.

## Migration

Confluent BAEC monolayers in 35-mm dishes were wounded with a razor blade, as described previously.<sup>(13)</sup> After the wounding, the cells were washed with PBS and then incubated with fresh BSA–DMEM alone or BSA–DMEM plus 1 nM bFGF and the desired concentrations of RA-VII. The cells were then incubated for a further 24 h, fixed with methanol, and stained with crystal violet. Cells that had migrated from the edge of the wound were counted as the mean of five fields per dish, and the values were expressed as the mean  $\pm$  SD of three dishes.

## Fluorescence staining of filamentous actin

Aliquots of BAEC ( $3 \times 10^4$ ) were plated in 35-mm dishes and cultured in 10% FCS–DMEM for 24 h. The medium was then changed to BSA–DMEM alone or BSA–DMEM containing RA-VII, and the cells were subsequently incubated for another 48 h. Next, the medium was changed to BSA–DMEM alone or BSA–DMEM containing 1 nM bFGF, after which the cells were incubated for another 1 h, washed three times with PBS, and fixed in 3.7% formaldehyde in PBS. The fixed cells were washed three times with PBS, and then with 0.1% Triton-X in PBS for 3 min at  $-30^\circ\text{C}$ . After being washed three times with PBS, they were finally incubated with 5  $\mu\text{g}/\text{mL}$  rhodamine-conjugated phalloidin in PBS containing 1% BSA at  $37^\circ\text{C}$  for 30 min, mounted, and observed microscopically using an LSM5 PACAL Laser Scanning Microscope (Carl Zeiss, Jena, Germany).

## Animal studies

All of the animal studies were reviewed and approved by the committee for animal study in our institute in accordance with established standards of humane handling.

## Mouse corneal micropocket assay

The mouse corneal micropocket assay and quantification of corneal neovascularization was carried out as described previously.<sup>(14)</sup> Briefly, a 0.3- $\mu\text{g}$  pellet of poly 2-hydrocetyl methacrylate (poly HEME, Sigma) with or without bFGF (80 ng) was implanted in the cornea of each of several Institute of Cancer Research (ICR) mice (Charles River Japan, Yokohama, Japan). From the day of implantation, the animals received a daily intraperitoneal injection of RA-VII (4 mg/kg) or vehicle. After 7 days, the animals were anesthetized and the vessels were then photographed. Quantification of neovascularization in the cornea was carried out by using NIH image software.

## Tumor growth in mice

Male C57Bl/6 J mice, 6–7 weeks old (Charles River Japan), were inoculated intradermally with 100  $\mu\text{L}$  of  $5 \times 10^6$  LLC cells/mL medium. Seven days after the injection, the animals were randomized into RA-VII (3 mg/kg/day), RA-VII (1.5 mg/kg/day) and control groups, with eight mice in each group. Mice in the RA-VII group were given a daily intraperitoneal injection of RA-VII at 3 mg/kg/day or 1.5 mg/kg/day, whereas the control mice received an equivalent volume of 0.5% gum arabic (in PBS) instead of RA-VII. Mice were monitored for weight loss and tumor progression. At day 14, the animals were killed, and paraffin

sections were prepared from the excised tumors. Tumor volume was calculated as  $1/2 \times \text{length} (\times \text{width})$ .<sup>(2)</sup>

## Immunohistochemistry for tumor vessels

For histochemical analysis, tumors were fixed immediately in 4% paraformaldehyde at  $4^\circ\text{C}$  overnight. Thereafter, the tumor tissues were dehydrated and paraffin-embedded. Immunostaining was carried out on 5- $\mu\text{m}$  tissue sections placed on super frost (Matsunami adhesive silane [MAS]-coated) glass slides. After deparaffinization in xylene and a graded alcohol series, the slides were used for immunohistochemical study. First, the tissue sections were pretreated with proteinase K for 15 min and then blocked for 10 min with Non-Specific Staining Blocking Reagent. After the blocking reagent had been removed, the sections were exposed to the primary antibody, rat antimouse CD31 (1:100), overnight at  $4^\circ\text{C}$ . The next day, they were washed with PBS and exposed to the secondary antibody, goat antirat IgG conjugated to biotin, at a dilution of 1 : 500 for 30 min. Labeling was visualized using a streptavidin–Cy3 conjugate (Sigma) at a dilution of 1:100. Thereafter, the sections were exposed to the primary antibody mouse antimouse  $\alpha\text{SMA}$  (1:200, Sigma) overnight at  $4^\circ\text{C}$ . The next day, they were washed with PBS and exposed for 30 min to secondary antibody, goat antimouse IgG conjugated to FITC. Thereafter, the sections were mounted with fluorescence-enhancing medium and observed under an Olympus IX70 microscope (Tokyo, Japan). Images were captured with an Olympus DP70 microscope. Vessel area was quantified in 20 fields in four sections. Total vessel area was given as a mean of eight fields and values were expressed as mean  $\pm$  SD of four fields.

## Terminal deoxynucleotidyl transferase-mediated nick-end labeling staining

After sections had been stained with anti-CD31 and streptavidin–Cy-3, they were washed in PBS and then incubated with equilibration buffer (TdT buffer) for 5 min. Thereafter, the sections were reacted with 16-dUTP-fluorescein in working-strength TdT for 60 min at  $37^\circ\text{C}$ . Distilled water was used instead of TdT for negative controls. As positive control, sections were reacted with DNase I for 15 min at  $37^\circ\text{C}$ . Stop-wash standard saline citrate (SSC) solution was used for 15 min to stop the reaction, whereafter the sections were washed in PBS and mounted. Sections were viewed with an Olympus IX70 microscope. Apoptotic cells were counted in a total of 20 fields (five fields in each of four sections) and expressed as the mean  $\pm$  SD per field.

## Cytotoxicity

Aliquots of LLC cells ( $1 \times 10^4$ ) or BAEC ( $1 \times 10^4$ ) were plated in a 96-well plate and cultured in 10% FBS–DMEM for 24 h. Thereafter, the medium was changed to 0.1% BSA in DMEM (BSA–DMEM) and the desired concentrations of RA-VII, RA-III, RA-V or water-soluble derivative. After a 24-h incubation, the cells were incubated with Tetra Color ONE for 4 h. The absorbance was then read at 450 nm.

## Calculations and statistical analysis

The statistical significance of differences between results was evaluated using the unpaired analysis of variance, and *P*-values

were calculated. A value of  $P < 0.05$  was accepted as statistically significant.

## Results

### Effects of RA-VII, its water-soluble derivative, RA-III and RA-V on the migration and proliferation of BAEC

First, we examined the effects of RA-VII, its water-soluble derivative, RA-III and RA-V on bFGF-stimulated migration of BAEC. All four compounds inhibited migration in a dose-dependent manner. Among the compounds tested at 10 nM, RA-VII inhibited migration most efficiently (Fig. 2).

We next examined the effect of each of the four compounds on bFGF-stimulated proliferation of BAEC. The difference in effect was more pronounced in this analysis. RA-VII (3 nM and 10 nM) significantly inhibited bFGF-stimulated proliferation of BAEC, whereas the other three compounds showed no such effect at the same concentrations tested (Fig. 3a–d). Similar results were obtained from cell counting and a BrdU incorporation assay (data not shown). VEGF-stimulated proliferation of HUVEC was also inhibited by RA-VII (Fig. 3e). Thus, the inhibitory effect of RA-VII was not specific to bFGF. As RA-VII showed the most profound effect on EC, we used it in the subsequent experiments.

### Effect of RA-VII on stress fiber formation in BAEC

As RA-VII binds to actin and induces a conformational change in actin structure,<sup>(12)</sup> we examined the effect of RA-VII on stress fiber formation. RA-VII caused aggregation of

actin around the nuclei in control BAEC (Fig. 4). bFGF induced the formation of stress fibers in BAEC, and RA-VII inhibited it (Fig. 4)

### Effect of RA-VII on mouse corneal angiogenesis

As migration and proliferation are indispensable properties of EC for angiogenesis,<sup>(1)</sup> we examined whether RA-VII could exhibit anti-angiogenic activity. We inoculated a pellet containing bFGF into the mouse cornea to induce angiogenesis. The daily intraperitoneal injection of RA-VII (4 mg/kg) for 7 days apparently inhibited this angiogenesis (Fig. 5a). Quantitative analysis confirmed the anti-angiogenic activity of RA-VII via this systemic administration (Fig. 5b).

### Effect of RA-VII on the growth of LLC cells inoculated into mice

As RA-VII showed significant anti-angiogenic activity in mice, we applied RA-VII to the treatment of tumors. LLC cells ( $5 \times 10^6$  cells) were inoculated subcutaneously into mice, and 1 week later RA-VII was injected intraperitoneally at a dose of 1.5 or 3 mg/kg daily for 7 days. The 50% lethal dose of RA-VII calculated using the Lichfield–Wilcoxon method was 16.5 mg/kg.<sup>(11)</sup> The administration of RA-VII at a dose of 1.5 mg/kg/day resulted in a significant reduction in tumor volume, 37, 49 and 43% at days 10, 12 and 14, respectively, after tumor inoculation. At 3 mg/kg/day the reduction was even more dramatic, being 61, 73 and 76%, respectively (Fig. 6a). After the 7-day treatment, we weighed the excised tumors. RA-VII significantly reduced the tumor weight in a dose-dependent manner (Fig. 6b). Animals were

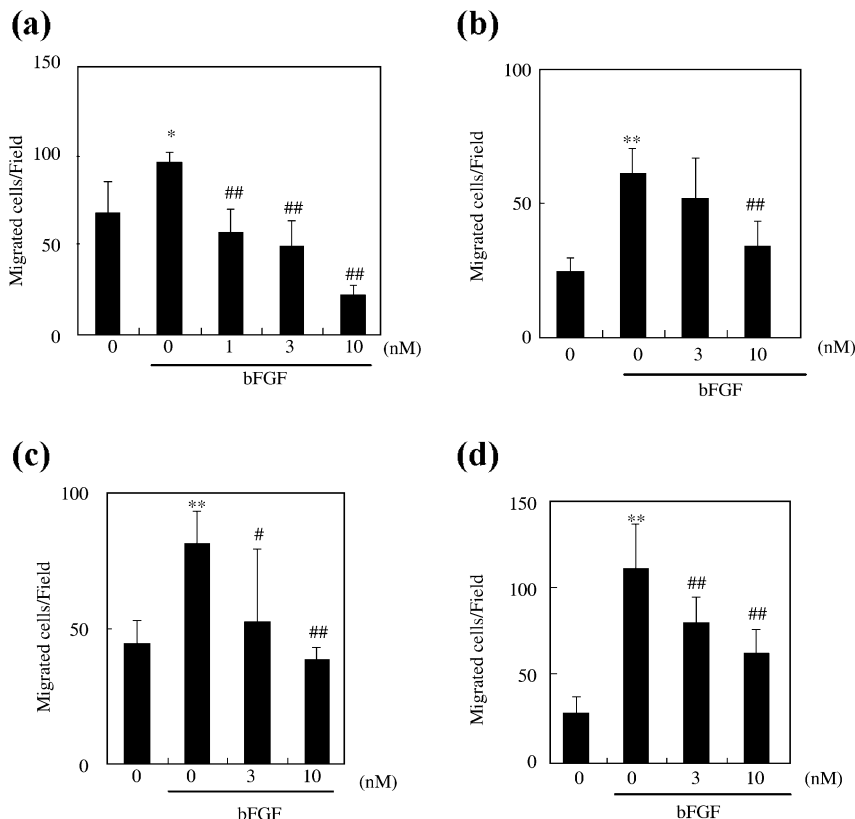


**Fig. 2.** Effect of RA-VII, its water-soluble derivative, RA-III and RA-V on the migration of bovine aortic endothelial cells (BAEC). The wound migration assay was carried out as described in Materials and Methods. BAEC were treated with the indicated concentrations of compounds with or without basic fibroblast growth factor (bFGF) (1 nM) for 24 h: (a) RA-VII (b) water-soluble derivative, (c) RA-III and (d) RA-V. The number of cells that migrated from the wound margin were counted and calculated as the mean of five fields per dish, and the values are expressed as the mean  $\pm$  SD of four dishes. \* $P < 0.05$ , \*\* $P < 0.01$  versus control; # $P < 0.05$ , ## $P < 0.01$  versus bFGF alone.

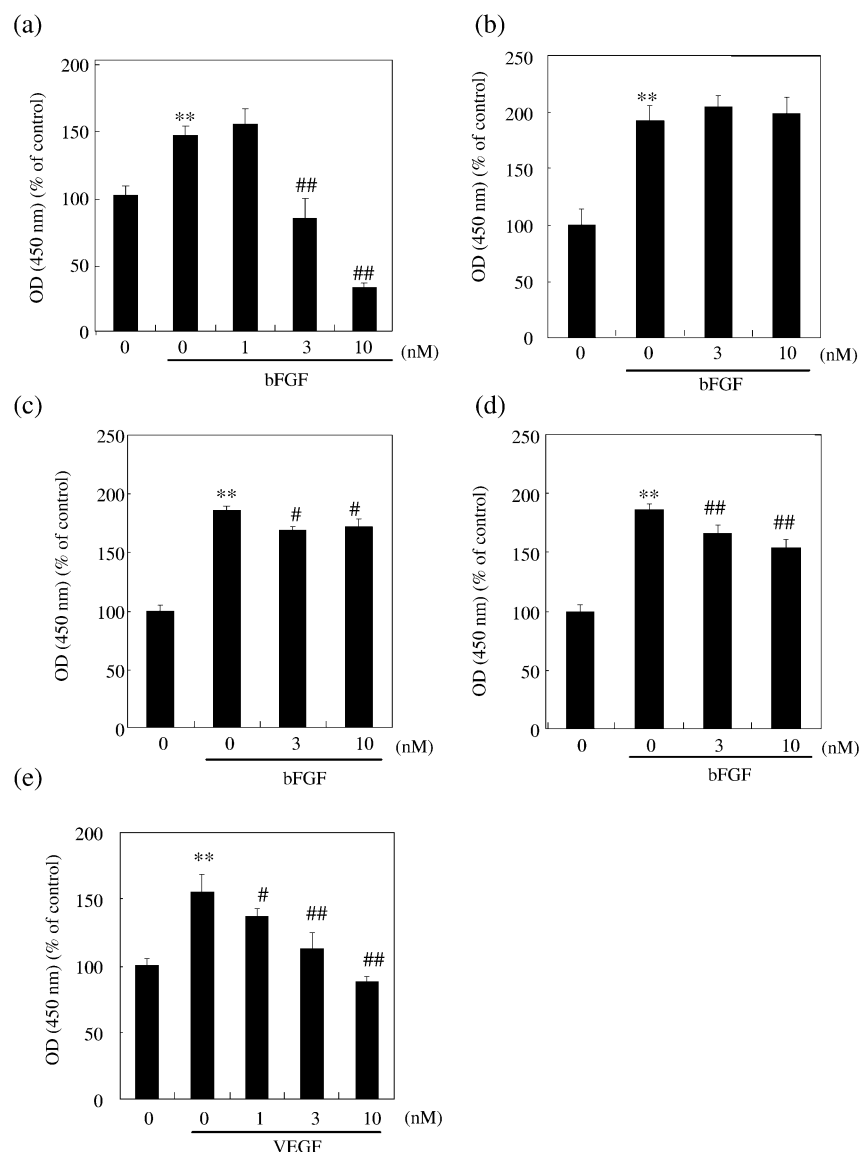


**Fig. 3.** Effect of RA-VII, water-soluble derivative, RA-III and RA-V on the proliferation of bovine aortic endothelial cells (BAEC). Cell proliferation was assessed using Tetra Color ONE as described in Materials and Methods. BAEC were treated with the indicated concentrations of compounds with or without basic fibroblast growth factor (bFGF) (1 nM) for 72 h. Cell proliferation is expressed as a percentage against the control (100%). (a) RA-VII, (b) water-soluble derivative, (c) RA-III and (d) RA-V. Values are expressed as the mean  $\pm$  SD of six samples. (e) Human umbilical vein endothelial cells (HUVEC) were treated with the indicated concentrations of compounds with or without vascular endothelial growth factor (VEGF) (1 nM) for 72 h. \*\* $P$  < 0.01 versus control; # $P$  < 0.05, ## $P$  < 0.01 versus bFGF alone.

well tolerated at both dosages of RA-VII, as no significant effects on bodyweight (Fig. 6c) or general wellbeing (data not shown) were observed.

#### Effect of RA-VII on tumor vessels

We examined tumor vessels by immunostaining for the EC marker CD31. CD31 immunostaining showed that vessels in the tumors of mice treated with vehicle were markedly dilated (Fig. 7a). Upon quantifying the luminal area of these vessels, we found that treatment with RA-VII at a dose of 1.5 or 3 mg/kg/day significantly reduced it (Fig. 7b). Although the tumor vessel area at a dose of 1.5 and 3 mg/kg/day was identical, the morphology of tumor vessels was quite different. Tumor vessels at a dose of 3 mg/kg/day were round, whereas those at a dose of 1.5 mg/kg/day showed sprouting (Fig. 7a).

In order to characterize the vessel wall structure, we carried out immunostaining with the mural cell marker  $\alpha$ -SMA. Round vessels at a dose of 3 mg/kg/day were

associated with mural cells, whereas sprouting vessels were not (Fig. 8a). Quantitative analysis revealed that more tumor vessels were associated with mural cells in mice treated with 3 mg/kg/day of RA-VII (Fig. 8b)

#### Effect of RA-VII on apoptosis in tumor tissue

We then examined apoptosis in tumor tissue by terminal deoxynucleotidyl transferase-mediated nick-end labeling (TUNEL) staining. Most of the TUNEL-positive cells were tumor cells, and very few endothelial cells were TUNEL-positive even in the RA-VII-treated group (Fig. 9a). Quantitative analysis revealed that the number of TUNEL-positive tumor cells increased significantly in a dose-dependent manner (Fig. 9b).

As the apoptotic cells were mainly tumor cells, we examined the cytotoxic effect of RA-VII on LLC and BAEC. As shown in Fig. 10, RA-VII exhibited a cytotoxic effect on both cell lines, but the effect was much more pronounced in the case of the LLC.

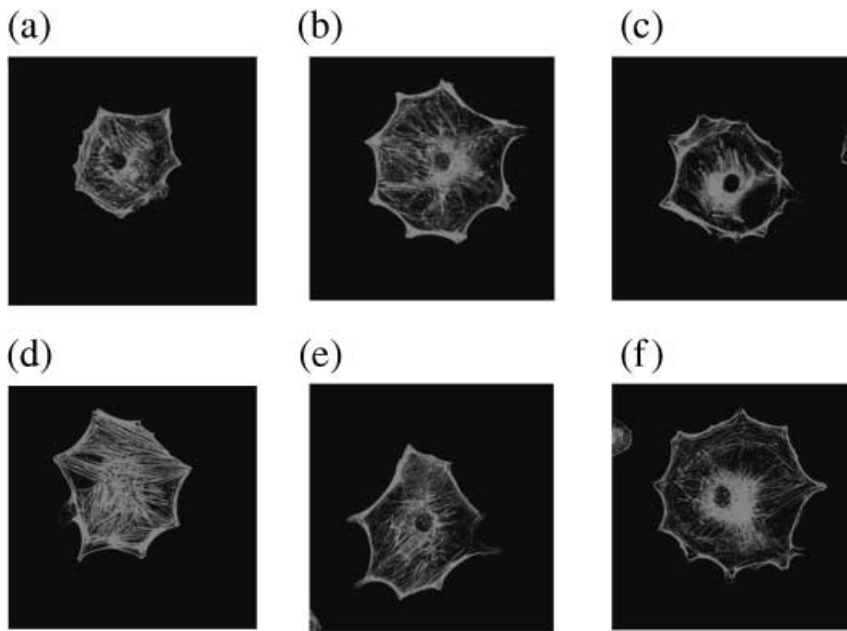


**Fig. 4.** Effect of RA-VII on the stress fiber formation of bovine aortic endothelial cells (BAEC). Stress fiber formation was observed by rhodamin-phalloidin staining as described in Materials and Methods. BAEC were cultured in 0.1% bovine serum albumin–Dulbecco’s modified Eagle’s medium with the indicated concentrations of RA-VII. After 48 h, the cells were incubated with or without basic fibroblast growth factor (bFGF) for 1 h. Thereafter, they were stained with rhodamine-phalloidin. The photos show fluorescent images of the cells. (a) Vehicle, (b) RA-VII (3 nM), (c) RA-VII (10 nM), (d) bFGF (1 nM), (e) bFGF (1 nM) + RA-VII (3 nM) and (f) bFGF (1 nM) + RA-VII (10 nM).

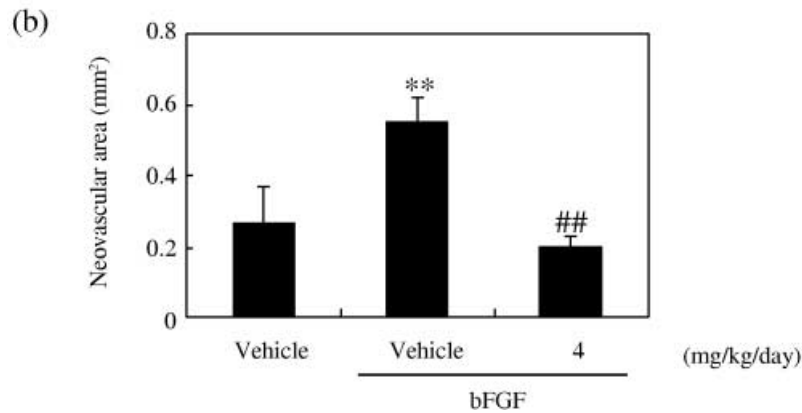
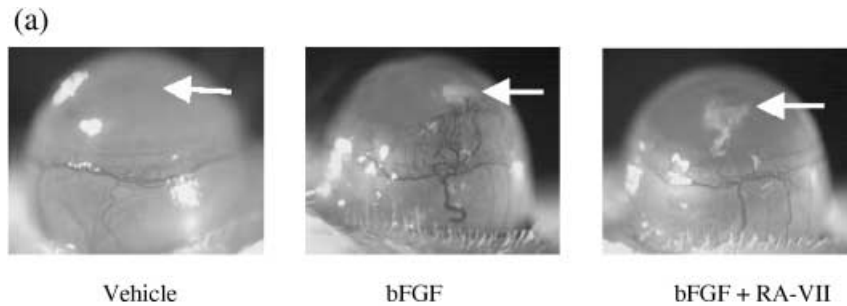


**Fig. 5.** Effect of RA-VII on angiogenesis in the mouse cornea. The effect of RA-VII on angiogenesis *in vivo* was assessed by conducting the mouse corneal micropocket assay, as described in Materials and Methods. (a) The photos show microscopic images of the corneas, with arrows indicating the sites where pellets were implanted. (b) Quantification of angiogenesis was carried out using NIH image software. Values are expressed as the mean  $\pm$  SD of five eyes, \*\* $P < 0.01$  versus vehicle; ##  $P < 0.01$  versus basic fibroblast growth factor (bFGF) alone.

## Discussion

Here we identified the anti-angiogenic activity of RA-VII and further applied it to the treatment of cancer in an animal model. We observed that daily administration of RA-VII at 1.5 mg/kg or 3.0 mg/kg was not toxic to mice but exhibited a significant anti-angiogenic and antitumor effect. Cytotoxic agents show anti-angiogenic activity when administered at doses substantially lower than the maximum tolerated dose on a continuous or very frequent schedule. Such scheduling

of cytotoxic agents, so-called metronomic chemotherapy, has been shown to exert significant therapeutic efficacy in various tumor models with very limited toxicity.<sup>(15)</sup> Thus, our present protocol with RA-VII is regarded as one with a metronomic anti-angiogenic schedule.

Interestingly, we observed a dose-responsive antitumor effect when mice were treated with RA-VII at 1.5 mg/kg/day or 3.0 mg/kg/day. The decrease in luminal tumor vessel area was equivalent between these two doses; however, a striking difference was found in that tumor vessels in animals treated

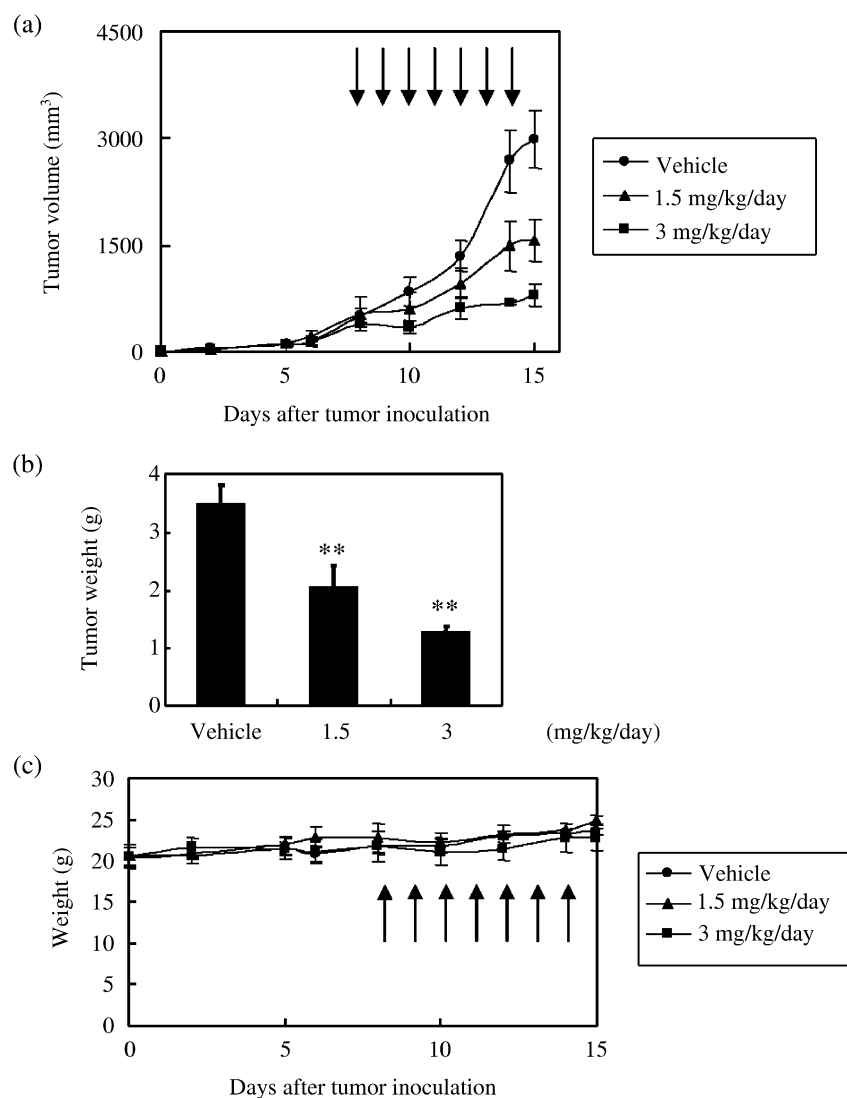


**Fig. 6.** Effect of RA-VII on tumor growth in mice. Lewis lung carcinoma (LLC) cells were inoculated into C57/Bl6 mice, and tumor growth was observed. From 8 days after the inoculation, RA-VII was administered every day for 7 days. At day 15, the animals were killed and tumors excised. (a) Tumor progression, (b) weight of excised tumors, and (c) bodyweight. Arrows indicate times of RA-VII injection. Values are expressed as mean  $\pm$  SD of four animals. \* $P < 0.05$ , \*\* $P < 0.01$  versus vehicle.

with 3.0 mg/kg/day of RA-VII were round, whereas those in animals with 1.5 mg/kg/day showed sprouting. Moreover, immunostaining for  $\alpha$ SMA indicated that tumor vessels in the animals treated with 3.0 mg/kg/day of RA-VII were associated with  $\alpha$ SMA-positive mural cells. These characteristic features indicate that tumor vessels in animals treated with 3.0 mg/kg/day of RA-VII became mature, whereas those in the mice treated with 1.5 mg/kg/day were still immature.

Maturation of tumor vessels is regarded as an important component in anti-angiogenic treatment, especially in the case of blockade of VEGF signaling.<sup>(16)</sup> When bevacizumab is administered as a monotherapy, it does not yield long-term survival benefit. In contrast, when given in combination with conventional chemotherapy, bevacizumab produces an increase in survival in colorectal cancer patients.<sup>(5)</sup> The mechanism of this combination effect is explained by the maturation of tumor vessels caused by bevacizumab treatment.<sup>(17)</sup> The maturation of vessels is thought to produce an increase in tumor blood flow and therefore enhanced delivery of anticancer agents to the cancer cells that surround the 'mature' vessels.<sup>(16,17)</sup> However, the maturation of tumor vessels has not been previously documented to occur in metronomic chemotherapy.

Our present study revealed that 3.0 mg/kg/day of RA-VII induced the maturation of tumor vessels. The mechanism as to how this dose of RA-VII induces vascular maturation remains to be clarified. However, the important point is that the cytotoxic effect of RA-VII on cancer cells judged by TUNEL staining was remarkable at the dose of 3.0 mg/kg/day. Thus, without being combined with selective anti-angiogenic drugs such as bevacizumab, RA-VII can induce the maturation of tumor vessels, which increases its cytotoxicity toward cancer cells as a monotherapy. We therefore propose that a careful dose setting of RA-VII is crucial to obtain therapeutic superiority through the maturation of tumor vessels and to obtain a better delivery of this drug to cancer cells. Understanding of the significance of tumor vessel maturation may lead to a novel approach to improve the efficacy of metronomic chemotherapy.

## Acknowledgment

This work was supported by the 21st Century COE Program Special Research Grant 'The Center for Innovative Therapeutic Development for Common Diseases'.

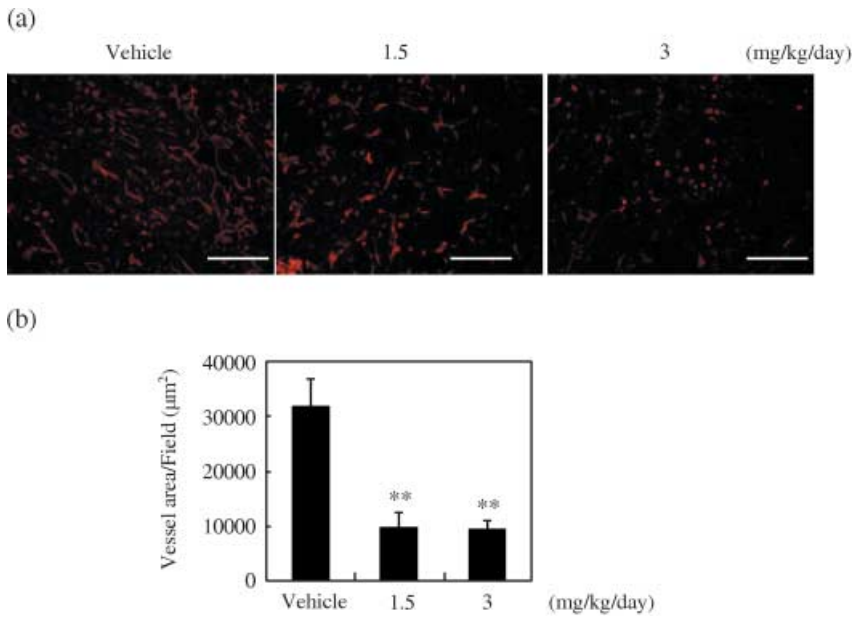


**Fig. 7.** Effect of RA-VII on tumor angiogenesis. Tumor sections obtained on day 15 were stained for CD31 as described in Materials and Methods. (a) Fluorescent images of CD31-positive cells. Scale bars = 200 μm. (b) Quantification of vascular luminal area of the tumor. Vessel areas were calculated as the mean of five fields per section and the values are expressed as the mean ± SD of four sections. \*\* $P < 0.01$  versus vehicle.

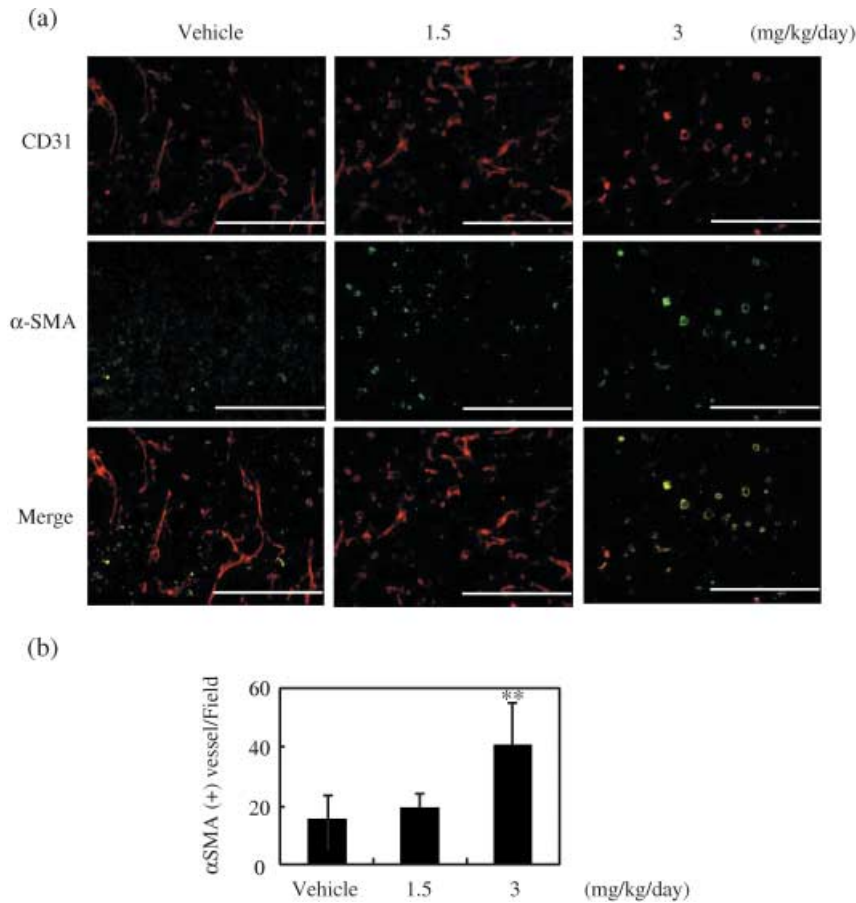


**Fig. 8.** Effect of RA-VII on tumor vessel maturation. Tumor sections obtained on day 15 were stained for CD31 and α-smooth muscle actin (αSMA), as described in Materials and Methods. CD31 was visualized using biotinylated anti-CD31 and a streptavidin-Cy3 conjugate, and αSMA was visualized with mouse anti-αSMA and fluorescein-isothiocyanate-conjugated goat antimouse antibody. (a) Fluorescent images of CD31 and αSMA. Scale bars = 200 μm. (b) Quantification of αSMA-associated mature vessels was carried out by counting CD31<sup>+</sup>/αSMA<sup>+</sup> vessels per field. Their numbers were counted and calculated as the mean of five fields per section, and the values expressed as the mean ± SD of four sections. \*\* $P < 0.01$  versus vehicle.



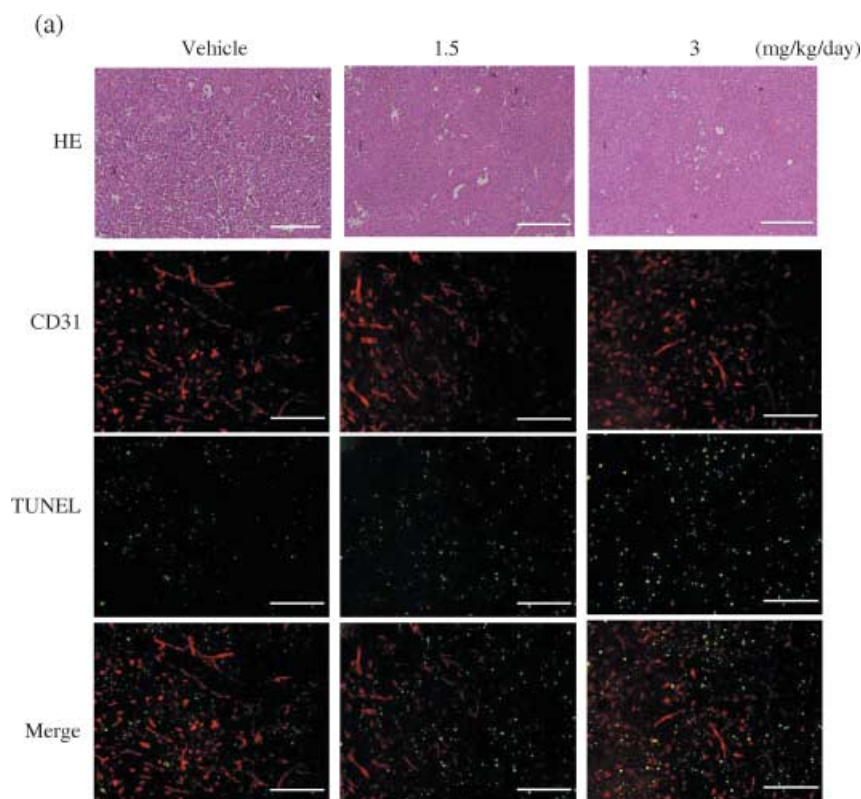


**Fig. 9.** Effect of RA-VII on apoptosis in tumor tissues. Tumor sections obtained from mice on day 15 after inoculation were stained for hematoxylin and eosin (H&E), CD31 and the terminal deoxynucleotidyl transferase-mediated nick-end labeling (TUNEL) reaction. CD31 was visualized using biotinylated anti-CD31 and a streptavidin-Cy3 conjugate, and TUNEL used a 16-dUTP-fluorescein conjugate. (A) H&E staining, fluorescent images of CD31 and TUNEL. Scale bars = 200  $\mu$ m. (B) Quantification of apoptotic cell numbers. Apoptotic cells were counted and calculated as the mean of five fields per section and the values expressed as the mean  $\pm$  SD of four sections. \*\* $P$  < 0.01 versus vehicle.

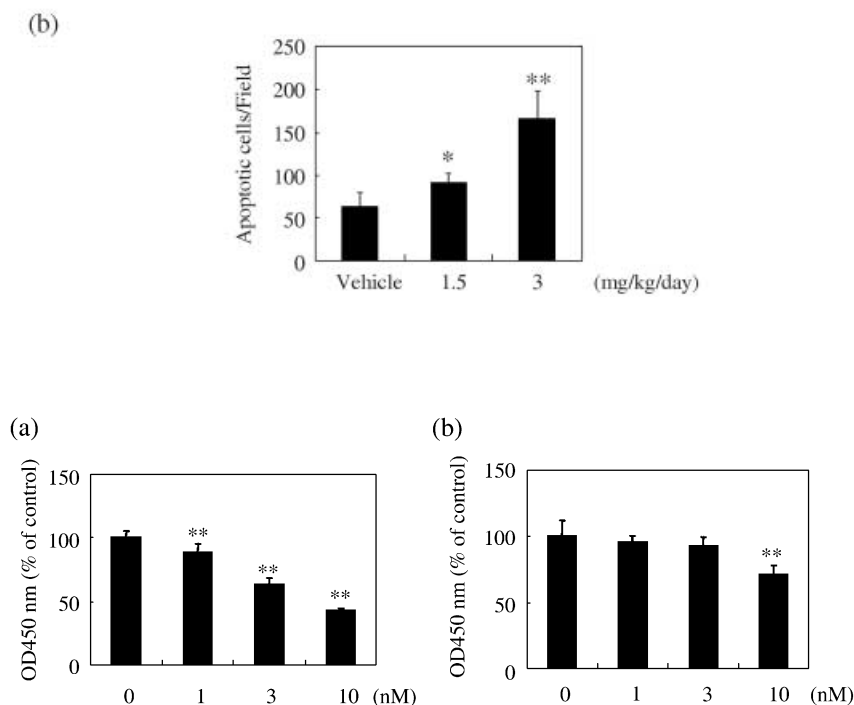


**Fig. 10.** Cytotoxic effect of RA-VII on Lewis lung carcinoma (LLC) cells and bovine aortic endothelial cells (BAEC). Cytotoxicity was assessed using Tetra Color ONE, as described in Materials and Methods. (a) LLC or (b) BAEC were treated with the indicated concentrations of RA-VII for 24 h. Cytotoxicity is expressed as a percentage against the control (100%). Values are expressed as the mean  $\pm$  SD of six samples. \* $P$  < 0.05, \*\* $P$  < 0.01 versus control.

## References

- Hanahan D. Signaling vascular morphogenesis and maintenance. *Science* 1997; **277**: 48–50.
- Falkman J. Angiogenesis in cancer, vascular, rheumatoid and other disease. *Nat Med* 1995; **1**: 27–31.
- Baluk P, Hashizume H, McDonald DM. Cellular abnormalities of blood vessels as targets in cancer. *Curr Opin Genet Dev* 2005; **15**: 102–11.
- Folkman J. Tumor angiogenesis: therapeutic implications. *N Engl J Med* 1971; **285**: 1182–6.
- Hurwitz H, Fehrenbacher L, Novotny W *et al.* Bevacizumab plus irinotecan, fluorouracil, and leucovorin for metastatic colorectal cancer. *N Engl J Med* 2004; **350**: 2335–42.
- Folkman J. Angiogenesis inhibitors: a new class of drugs. *Cancer Biol Ther* 2003; **2** (4 Suppl. 1): S127–33.
- Brunton VG, MacPherson IR, Frame MC. Cell adhesion receptors,

- tyrosine kinases and actin modulators: a complex three-way circuitry. *Biochim Biophys Acta* 2004; **1692**: 121–44.
- 8 Vicente-Manzanares M, Webb DJ, Horwitz AR. Cell migration at a glance. *J Cell Sci* 2005; **118**: 4917–19.
  - 9 Robinson DN, Swudich JA. Towards a molecular understanding of cytokinesis. *Trends Cell Biol* 2000; **10**: 228–37.
  - 10 Abe M, Inoue D, Matsunaga K *et al.* Goniodomin A, an antifungal polyether macrolide, exhibits antiangiogenic activities via inhibition of actin reorganization in endothelial cells. *J Cell Physiol* 2002; **190**: 109–16.
  - 11 Itokawa H, Takeya K, Mori N, Hamanaka T, Sonobe T, Mihara K. Isolation and antitumor activity of cyclic hexapeptides isolated from *Rubiae radix*. *Chem Pharm Bull* 1984; **32**: 284–90.
  - 12 Fujiwara H, Saito S, Hitotsuyanagi Y, Takeya K, Ohizumi Y. RA-VII, a cyclic depsipeptide, changes the conformational structure of actin to cause G<sub>2</sub> arrest by the inhibition of cytokinesis. *Cancer Lett* 2004; **209**: 223–9.
  - 13 Sato Y, Rifkin DB. Autocrine activities of basic fibroblast growth factor: regulation of endothelial cell movement, plasminogen activator synthesis, and DNA synthesis. *J Cell Biol* 1988; **107**: 1199–205.
  - 14 Watanabe K, Hasegawa Y, Yamashita H *et al.* Vasohibin as an endothelium-derived negative feedback regulator of angiogenesis. *J Clin Invest* 2004; **114**: 898–907.
  - 15 Kerbel R, Kamen BA. The anti-angiogenic basis of metronomic chemotherapy. *Nat Rev Cancer* 2004; **4**: 423–36.
  - 16 Jain RK. Normalization of tumor vasculature: An emerging concept in antiangiogenic therapy. *Science* 2005; **307**: 58–62.
  - 17 Willett CG, Boucher Y, di Tomaso E *et al.* Direct evidence that the VEGF-specific antibody bevacizumab has antivascular effects in human rectal cancer. *Nat Med* 2004; **10**: 145–7.